Optical isolator based on chiral light-matter interactions in a ring resonator integrating a dichroic magneto-optical material

Yuma Kawaguchi, Mengyao Li, Kai Chen, Vinod Menon, Andrea Alù, and Alexander B. Khanikaev

View Online

Export Citation

CrossMark
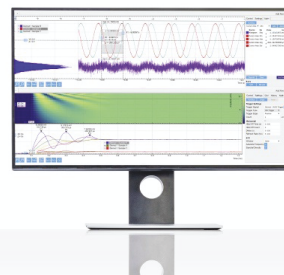
Optical isolator based on chiral light-matter interactions in a ring resonator integrating a dichroic magneto-optical material

View Online   Export Citation   CrossMark

Yuma Kawaguchi,[1] (iD) Mengyao Li,[1,2,3] Kai Chen,[1,2,3] Vinod Menon,[2,3] (iD) Andrea Alù,[1,2,4] (iD)
and Alexander B. Khanikaev[1,2,3,a)] (iD)

AFFILIATIONS

[1]Department of Electrical Engineering, City College of the City University of New York, 160 Convent Avenue, New York,
New York 10031, USA
[2]Department of Physics, City College of the City University of New York, 160 Convent Avenue, New York, New York 10031, USA
[3]Physics Program, Graduate Center of the City University of New York, New York, New York 10016, USA
[4]Photonics Initiative, Advanced Science Research Center, City University of New York, New York, New York 10031, USA

Note: This Paper is part of the APL Special Collection on Metastructures: From Physics to Applications.
[a)]Author to whom correspondence should be addressed: akhanikaev@ccny.cuny.edu

ABSTRACT

Nonreciprocal optical devices based on magneto-optical ferrites in their low-loss regimes have been widely investigated as a promising platform for integrated photonics. Nonreciprocity in such devices originates from circular birefringence, leading to frequency splitting of forward and backward modes and, as a result, nonreciprocal transmission. In this paper, we propose an alternative approach to realize nonreciprocal devices based on magneto-optical circular dichroism and relying on the very presence of optical absorption. Our approach relies on the phenomenon of spin-Hall effect of light, which gives rise to chiral near field interactions of light carrying transverse angular momentum with matter, which, in lossy regimes, yields a disparate absorption for forward and backward optical modes. As an example of practical application, we design an optical isolator based on ring resonator integrating Ce:YIG ferrite, and we demonstrate isolation near 880 nm absorption line due to the ionic electric dipole transition. A Ce:YIG film asymmetrically placed on the inner side of the ring yields different critical coupling conditions due to the chiral nature of evanescent light for forward and backward waves, leading to nonreciprocal absorption and transmission. The proposed approach to nonreciprocity may significantly broaden the possible choice of magneto-optical materials for nonreciprocal devices, enabling operation even in lossy regimes.

Published under an exclusive license by AIP Publishing. https://doi.org/10.1063/5.0057558

Non-reciprocal devices, such as optical isolators and circulators, play a critical role in optical applications by enabling unidirectional propagation of optical signals.[1] A variety of approaches to nonreciprocity, e.g., nonlinear optics and spatiotemporal modulation[2–7] and Weyl insulator,[8] have been proposed to achieve optical nonreciprocity, but the traditional approach based on magneto-optical (MO) materials remains an industry standard.[9–20] Recently, due to the increasing importance of integrated photonics, a number of on-chip nonreciprocal devices consisting of MO garnets, such as bismuth substituted yttrium iron garnet (Bi:YIG) and cerium substituted YIG (Ce:YIG), have been proposed.[21–24] For integrated photonics, it is important that thin MO garnets can be fabricated in high crystal quality on semiconductor substrates.[16,21,25] Specifically, integrated ring resonators with high quality (Q-) factors have been shown as a promising platform,[26–34] and non-reciprocal MO ring resonators and isolators on silicon were experimentally demonstrated,[10,13,35–37] yielding a large isolation ratio due to frequency splitting caused by the Faraday effect.

The nonreciprocal response of optical devices relies on a specific gyroelectric form of the permittivity tensor of MO materials in the presence of a magnetic field, which, for the field applied in the y-direction, can be expressed as

$$\hat{\varepsilon} = \begin{pmatrix} \varepsilon'_{xx} + i\varepsilon''_{xx} & 0 & \varepsilon'_{xz} + i\varepsilon''_{xz} \\ 0 & \varepsilon'_{yy} + i\varepsilon''_{yy} & 0 \\ -\varepsilon'_{xz} - i\varepsilon''_{xz} & 0 & \varepsilon'_{zz} + i\varepsilon''_{zz} \end{pmatrix}, \quad (1)$$

where the off diagonal components reflect the magnetization-induced optical activity of the material. A traditional approach to nonreciprocity with MO materials relies on circular birefringence, i.e., the Faraday effect, providing frequency splitting due to the imaginary part of the off diagonal terms ε_{xz}'' in the permittivity tensor (1). The device operation based on this principle typically shows best performance in a lossless (or nearly lossless) regime ($\varepsilon_{xx}'' \approx 0$ and $\varepsilon_{xz}' \approx 0$), and its performance deteriorates when either direct material loss (described by ε_{xx}'') or circularly dichroic loss (described by ε_{xz}') increases. This limits the application of most ferrite materials, which are typically lossy across most parts of the optical spectrum. As an example, for optical telecommunication wavelengths, the material of choice is Ce:YIG due to its small loss. However, losses in Ce:YIG start to dramatically increase for shorter wavelengths. In fact, in the most extreme scenario, the off diagonal permittivity tensor component can become purely real, implying a purely dichroic MO regime. Thus, Faraday rotation does not occur in such a regime, but light of opposite handedness experiences different absorption. Here, we demonstrate that nonreciprocal devices can be designed to operate in such purely dichroic regimes.

Our concept relies on the spin-Hall effect of light and the chiral nature of evanescent fields[38–40] of guided waves [Figs. 1(a) and 1(b)] and a specific chiral interaction of such field with dichroic MO materials. As a practical example, we design a nonreciprocal device formed by a waveguide coupled to a ring resonator, where such chiral light-matter interactions give rise to the different critical coupling conditions for forward and backward propagating waves and, as a result, to nonreciprocal absorption and transmission.

In what follows, we use Ce:YIG, which exhibits the Ce^{3+}–Fe^{3+} electric dipole transition at 880 nm,[41,42] at this wavelength, it is characterized by a purely dichroic permittivity tensor with components $\varepsilon_{xx} = \varepsilon_{zz} = \varepsilon_{xx}' + i\varepsilon_{xx}'' = 5.4 + i0.04$ and $\varepsilon_{xz} = \varepsilon_{xz}' + i\varepsilon_{xz}'' = 0.04$, which were measured experimentally for Ce:YIG grown by laser deposition.[43] The proposed isolator based on the ring resonator is illustrated in Fig. 1(c). Silicon nitride (SiN) was chosen as the material for both waveguide and ring, in order to avoid material loss for the wavelength of choice (880 nm). Importantly, the Ce:YIG film has a refractive index ($n = 2.32$), higher than the one of SiN ($n = 2$), and thus was designed to be thin enough so that the optical energy is confined within the waveguide/ring system and does not leak out due to
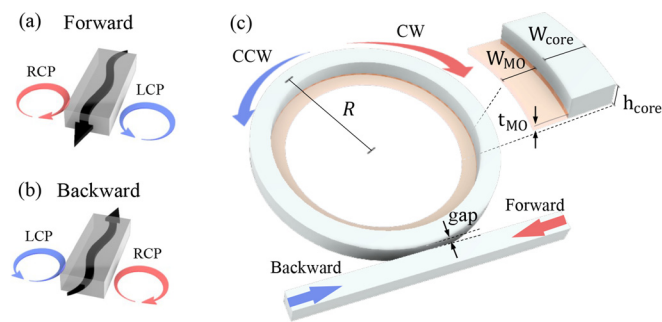

FIG. 1. (a) and (b) Schematics of the chirality of evanescent fields sustained by propagating waves in an optical waveguide for (a) forward and (b) backward directions. (c) Schematic model of the proposed isolator based on a ring resonator integrating a dichroic MO material. The MO ferrite film is placed on the inner side of the ring in order to break the symmetry and to give rise to chiral interactions of the propagating modes with the circularly dichroic ferrite.

excessive coupling to Ce:YIG. At the same time, this ensured that the Ce:YIG film causes only a weak perturbation to the modes of the ring resonator, yet sufficient for the nonreciprocal device operation.

The MO film, magnetized by a magnetic field perpendicular to the plane of the structure (y-direction), is placed only on the inner side of the ring resonator [Fig. 1(c)]. The propagating TE waves in the waveguide are known to be characterized by rotating (left- or right-handed) polarization of the evanescent in-plane (xz-plane) field on the sides of the waveguide,[44] as schematically indicated in Figs. 1(a) and 1(b). Importantly, reversal of the propagation direction leads to the reversal of the handedness of the near field. As shown below, a combination of this direction-dependent chirality of the near field with the dichroic response of the MO film yields a directional dichroic response, i.e., gives rise to different absorption rates of modes propagating in two opposite (forward and backward) directions.

We begin our analysis by considering a waveguide loaded by a MO film on one side, with the field distribution shown in Fig. 2(a), and whose modes will be used to study the modes of the ring resonator. As an illustration, Figs. 2(b) and 2(c) show that indeed, due to the spin-Hall effect of light, the forward propagating mode in the waveguide sustains predominantly left-handed circularly polarized (LCP) near field in the propagation plane on the right side and a right-handed circularly polarized (RCP) near field on the left side. For the backward propagating mode, the handedness of the field is reversed. We note that for the ring resonator geometry, this would indicate opposite handedness in the near field on the inner and outer sides of the resonator [Fig. 1(c)].

As a consequence of such chiral near field, an MO film placed on the left side of the waveguide will predominantly perceive the RCP near field of the forward propagating modes and the LCP near field for the backward propagating mode, giving rise to different absorption for forward and backward modes due to the circularly dichroic loss.

The nonreciprocal attenuation loss in the waveguide can be calculated using a coupled mode theory (CMT),[45,46] based on the modal profile obtained using first-principles finite-element (FEM) modeling. Two-dimensional simulations for the cross section of the SiN ($\varepsilon_{SiN} = 4$) waveguide and Ce:YIG film ($\varepsilon_{MO} = 5.4 + i0.04$) on a SiO$_2$ ($\varepsilon_{SiO2} = 2.1$) substrate have been performed using the FEM tool COMSOL Multiphysics (RF Module) in order to obtain the electric field distribution of the modes. The field distributions at 880 nm are shown in Fig. 2 for modes propagating out of the xy-plane, and clearly showing the chirality of the field, where LCP [Fig. 2(b)] and RCP [Fig. 2(c)] fields are localized on the opposite sides of the waveguide.

The correction to the wavenumber due to the addition of MO Ce:YIG film was obtained using CMT from the fields calculated in COMSOL Multiphysics. Due to the dichroism in the MO film, the major correction is to the imaginary part of the propagation constant, which, for forward ($+$) and backward ($-$) propagating waves, can be expressed as $Im(\beta_{+/-}) = \alpha \mp \Delta/2$, indicating disparate nonreciprocal loss for the two cases, where $\alpha = Im(n_{eff}\frac{2\pi}{\lambda})$ and

$$\Delta = \frac{\beta_0\epsilon_0}{W_0}\int_{MO} dS\left[\left(|E_{RCP}|^2 - |E_{LCP}|^2\right)Im[\varepsilon_{RCP} - \varepsilon_{LCP}]\right]. \quad (2)$$

Here, the energy of the (unperturbed) guided mode is given by $W_0 = \int dS\left[|E_0(r)|^2\varepsilon_0\varepsilon_s(r)\right]$, $\boldsymbol{E}_0$ is the normalized electric field of the modes, and $\varepsilon_s(r)$ is the relative permittivity.
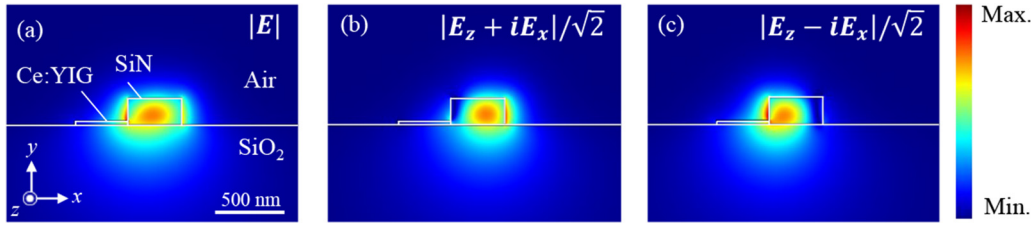
FIG. 2. Electrical distribution in the cross section of the waveguide in Fig. 1(a) at $\lambda = 880$ nm in the xy plane ($k = +k_z$). The width and height of the SiN waveguide are $w_{core} = 400$ nm and $h_{core} = 200$ nm, respectively. The thickness of Ce:YIG film is $t_{MO} = 30$ nm, and the width is $w_{MO} = 400$ nm, the same as the SiN waveguide. (a) Normalized electrical fields, (b) LCP electrical fields in the xz plane, and (c) RCP electrical fields in the xz plane.

The in-plane circularly polarized electric field components in Eq. (2) are defined as $E_{LCP} = (E_z + iE_x)/\sqrt{2}$ and $E_{RCP} = (E_z - iE_x)/\sqrt{2}$. The difference in the permittivity perceived by LCP ($\varepsilon_{LCP} = \varepsilon_{xx} + i\varepsilon_{xz}$) and RCP near fields ($\varepsilon_{RCP} = \varepsilon_{xx} - i\varepsilon_{xz}$) in Eq. (2) can be expressed as $\varepsilon_{LCP} - \varepsilon_{RCP} = 2\varepsilon'_{xz}$. The non-dichroic attenuation α originates from the diagonal part of the permittivity tensor and is the same for forward and backward modes. Finally, the attenuation coefficients $\text{Im}(\beta_{+/-})$ are evaluated by integration of the fields extracted from FEM solver and were found to be $\text{Im}(\beta_+) = 226$ 1/m for the forward and $\text{Im}(\beta_-) = 3760$ 1/m for the backward propagating modes. Details about the CMT are provided in the supplementary material.

Now we consider a ring resonator formed by bending the waveguide into a ring such that the Ce:YIG film is on the inner side of the ring. In this case, the difference in attenuation between forward and backward guided modes translates into different absorption rates for clockwise (CW) and counterclockwise (CCW) modes of the ring resonator [see Fig. 1(c)], which can be used to different critical coupling conditions for these modes. Thus, to achieve nonreciprocal transmission based on this mechanism, we consider the ring to be side-coupled evanescently to a SiN (without garnet) waveguide, which will provide two ports to couple to the ring-resonator [Figs. 1(c) and 3]. The transmission through the system via forward (+) and backward (−) propagating modes in the waveguide can then be analyzed with the use of CMT[27]

$$T_{+/-} = \frac{a_{+/-}^2 - 2a_{+/-}r\cos(\varphi) + r^2}{1 - 2a_{+/-}r\cos(\varphi) + (a_{+/-}r)^2}, \quad (3)$$

where $a_{+/-} = e^{-\text{Im}(\beta_{+/-})L}$ correspond to CW/CCW modes of the nonreciprocal ring resonator excited by forward/backward modes in the waveguide, respectively, $L = 2\pi R$ is the round trip length in the resonator, and the phase $\varphi = \text{Re}(\beta_{+/-})L$ accounts for the propagation in the ring. We note that there is no difference in φ between CCW and CW waves, since $\text{Re}(\beta_+) = \text{Re}(\beta_-)$, thus in our case (as opposed to the conventional approach based on MO circular dichroism), the resonances for forward and backward modes remain spectrally degenerate even in the presence of magnetization. The self-coupling coefficient r in Eq. (3) satisfies the relation $r^2 + \kappa^2 = 1$, where κ is the cross coupling coefficient describing the coupling strength between the ring and the waveguide. Therefore, the coefficient r is independent from material loss, and it can be adjusted by tuning the gap between the waveguide and the ring. The critical coupling condition for the backward propagating mode in the system is achieved when $r = a_-$, in which case backward transmission through the system vanishes $T_- = 0$. However, in the case of a dichroic ring resonator, this condition cannot be satisfied simultaneously for the case of forward propagating mode due to the different loss experienced by CW and CCW modes in the ring resonator $a_+ \neq a_-$, thus enabling transmission of the forward mode. As a result, the system operates as an isolator.
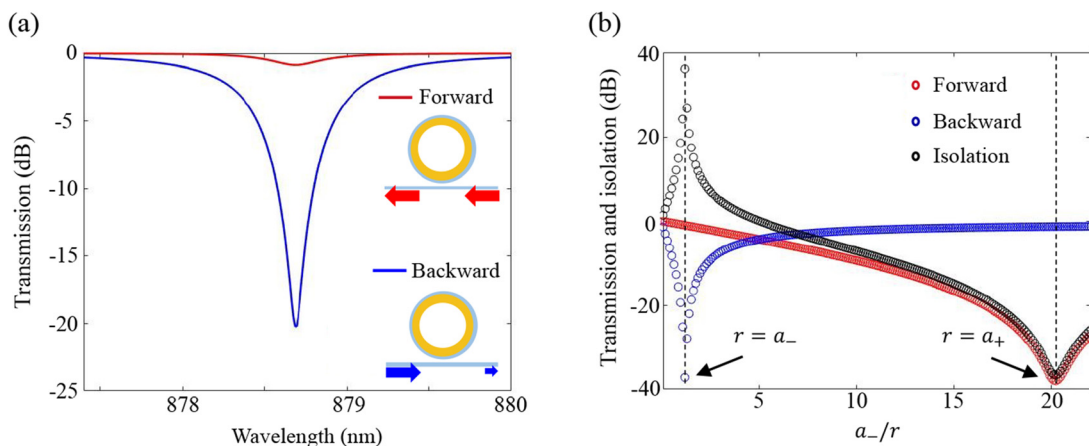

FIG. 3. (a) Transmission spectra passing through the ring resonator. The parameters are $L = 2\pi R$, $R = 8$ μm, and $r = 0.98a_-$. (b) The dependence of transmission and isolation from the ratio a_-/r-ratio at resonance wavelength $\lambda_{res} = 878.7$ nm. The maximal isolation is achieved near critical coupling conditions.

The transmission through the dichroic ring resonator near one of its resonances ($\lambda_{res} = 878.7$ nm) in the forward and backward directions as calculated from the CMT is shown in Fig. 3. The difference in transmission intensity stemming from the MO dichroic response between forward and backward directions is close to 20 dB. Notably, there is no spectral difference between the corresponding CW and CCW resonances, as it would be expected in the case of nonreciprocity based on MO circular birefringence.[36,37]

We note that the thickness of the MO film and its positioning play crucial role in the design and should be optimized to be thick enough to yield a sufficient dichroic response. On the other hand, if the MO layer is too thick, it will excessively perturb the guided modes, in which case they start to leak into the Ce:YIG leading to excessive losses and shift spectrally. In the case of the positioning of the MO film at the bottom of the waveguide/ring, which is more fabrication friendly design, we found the optimal thickness to be 30 nm.

In our case, to take advantage of the enhanced dichroic loss, the resonance of the ring resonator was tuned to be spectrally close to the Ce^{3+}–Fe^{3+} electric dipole transition in Ce:YIG. By tuning the gap between the waveguide and the ring resonator, the system was optimized to operate at the near-critical coupling condition for backward excitation (coupling to the CCW mode of the ring) $r = 0.98a_-$. For this case, the transmission at the resonance wavelength ($\lambda_{res} = 878.7$ nm) was -0.861 and -20.2 dB for the forward and backward directions, respectively. The $\sim$20 dB isolation can be farther increased by coming closer to the critical coupling condition ($r = a_-$), but at the cost of lower forward transmission due to stronger coupling of the forward propagating waveguide mode to the CW mode of the ring resonator [Fig. 3(b)]. For the case shown in Fig. 3(a), the forward propagating signal only slightly couples to the ring resonator, and this coupling is still far from critical, which yields relatively high transmission of $\sim$82%.

We note that the proposed approach to nonreciprocity envisions even broader range of applications for systems with photoinduced circular dichroism such as 2D transition metal dichalcogenides.[47] In this case, one can envisage the possibility of an all-optical control of nonreciprocity such as switching of the direction of isolation. Nonetheless, the design based on 3D MO materials proposed here has its own benefits since it can be easier to fabricate by conventional nanolithography and deposition of the MO materials, and it does not require an external laser pump to induce a dichroic response. Thus, we believe that the proposed design will find its use in optical systems where the static nonreciprocal response suffices.

In summary, here we explored the possibility of realizing an optical isolator based on purely dichroic non-reciprocal (magneto-optical) response. The proposed device consists of an optical ring resonator loaded by a thin layer of Ce:YIG material on the inside and side-coupled to an optical waveguide. We numerically demonstrated strong isolation near the frequency of Ce^{3+}–Fe^{3+} electric dipole transition, for which the response of the MO material is purely dichroic. Unlike previous devices, whose functionality is based on circular birefringence and spectral splitting of the modes (and of the associated reflection maxima), here we rely on critical coupling conditions that differ for CW and CCW modes in the MO dichroic ring resonator. Thus, the critical coupling condition can be satisfied for one direction only, while the other one exhibits high transmission. The scheme used here shows possibility to reach isolation of $\sim$20 dB with forward transmission exceeding 80%.

We believe that the proposed principle based on MO dichroism can be useful to design isolators from the abundant variety of lossy MO materials, thus expanding the range of frequencies over which such materials can be applied. In addition, it may allow the use of materials that were so far disregarded due to their lossy character in various spectral domains. The same concept of nonreciprocal device operation can be applied in the microwave domain, where many ferrites exhibit strong dichroic responses, especially near ferromagnetic resonances, and have so far been avoided due to loss.

See the supplementary material for details of the perturbation theory and a numerical demonstration of an isolator based on a 2D COMSOL Multiphysics model.

DATA AVAILABILITY

The data that support the findings of this study are available from the corresponding author upon reasonable request.

REFERENCES

[1] V. Asadchy, M. S. Mirmoosa, A. Díaz-Rubio, S. Fan, and S. A. Tretyakov, Proc. IEEE **108**, 1684 (2020).
[2] M. A. Díez-Ajenjo and P. Capilla, J. Optom. **3**, 2 (2010).
[3] N. A. Estep, D. L. Sounas, J. Soric, and A. Alù, Nat. Phys. **10**, 923 (2014).
[4] H. Lira, Z. Yu, S. Fan, and M. Lipson, Phys. Rev. Lett. **109**, 033901 (2012).
[5] C. W. Peterson, W. A. Benalcazar, M. Lin, T. L. Hughes, and G. Bahl, Phys. Rev. Lett. **123**, 63901 (2019).
[6] D. L. Sounas and A. Alù, Nat. Photonics **11**, 774 (2017).
[7] L. D. Tzuang, K. Fang, P. Nussenzveig, S. Fan, and M. Lipson, Nat. Photonics **8**, 701 (2014).
[8] V. S. Asadchy, C. Guo, B. Zhao, and S. Fan, Adv. Opt. Mater. **8**, 36 (2020).
[9] Y. Shoji, K. Miura, and T. Mizumoto, J. Opt. **18**, 013001 (2016).
[10] E. Ishida, K. Miura, Y. Shoji, H. Yokoi, T. Mizumoto, N. Nishiyama, and S. Arai, Opt. Express **25**, 452 (2017).
[11] K. Fang, Z. Yu, V. Liu, and S. Fan, Opt. Lett. **36**, 4254 (2011).
[12] N. Liu, J. Zhao, L. Du, C. Niu, C. Sun, X. Kong, Z. Wang, and X. Li, Opt. Lett. **45**, 5917 (2020).
[13] T. Mizumoto, R. Baets, and J. E. Bowers, MRS Bull. **43**, 419 (2018).
[14] S. Fan, Y. Shi, and Q. Lin, IEEE Antennas Wireless Propag. Lett. **17**, 1948 (2018).
[15] A. B. Khanikaev and M. J. Steel, Opt. Express **17**, 5265 (2009).
[16] T. Fakhrul, S. Tazlaru, L. Beran, Y. Zhang, M. Veis, and C. A. Ross, Adv. Opt. Mater. **7**, 1900056 (2019).
[17] Y. Shoji and T. Mizumoto, Sci. Technol. Adv. Mater. **15**, 014602 (2014).
[18] J. Kim, M. C. Kuzyk, K. Han, H. Wang, and G. Bahl, Nat. Phys. **11**, 275 (2015).
[19] B. J. H. Stadler and T. Mizumoto, IEEE Photonics J. **6**, 1 (2014).
[20] D. Jalas, A. Petrov, M. Eich, W. Freude, S. Fan, Z. Yu, R. Baets, M. Popović, A. Melloni, J. D. Joannopoulos, M. Vanwolleghem, C. R. Doerr, and H. Renner, Nat. Photonics **7**, 579 (2013).
[21] Y. L. Li, T. Li, Q.-Y. Wen, F. Fan, Q.-H. Yang, and S. Chang, Opt. Express **28**, 21062 (2020).
[22] R. L. Espinola, T. Izuhara, M.-C. Tsai, R. M. Osgood, and H. Dötsch, Opt. Lett. **29**, 941 (2004).
[23] M. A. Serrano-Núñez, Y. Shoji, and T. Mizumoto, Appl. Phys. Express **13**, 062002 (2020).
[24] M. C. Onbasli, T. Goto, X. Sun, N. Huynh, and C. A. Ross, Opt. Express **22**, 25183 (2014).

[25]T. Goto, Y. Eto, K. Kobayashi, Y. Haga, M. Inoue, and C. A. Ross, J. Appl. Phys. **113**, 2 (2013).

[26]A. Li and W. Bogaerts, Photonics Res. **6**, 620 (2018).

[27]A. Yariv, IEEE Photonics Technol. Lett. **14**, 483 (2002).

[28]D. L. Sounas and A. Alù, ACS Photonics **1**, 198 (2014).

[29]Z. Zhang, M. Dainese, L. Wosinski, and M. Qiu, Opt. Express **16**, 4621 (2008).

[30]Q. Xu and M. Lipson, Opt. Express **15**, 924 (2007).

[31]F. Wen, B. Guo, Y. Geng, F. Yang, and B. Wu, Appl. Phys. Express **12**, 072011 (2019).

[32]P. Pintus, M. C. Tien, and J. E. Bowers, IEEE Photonics Technol. Lett. **23**, 1670 (2011).

[33]N. A. Estep, D. L. Sounas, and A. Alù, IEEE Trans. Microwave Theory Tech. **64**, 502 (2016).

[34]W. Bogaerts, P. de Heyn, T. van Vaerenbergh, K. de Vos, S. Kumar Selvaraja, T. Claes, P. Dumon, P. Bienstman, D. van Thourhout, and R. Baets, Laser Photonics Rev. **6**, 47 (2012).

[35]K. Shang, S. Cheung, B. Li, R. P. Scott, Y. Takumura, and S. J. B. Yoo, in Optics InfoBase Conference Paper (2014), Vol. 3.

[36]L. Bi, J. Hu, P. Jiang, D. H. Kim, G. F. Dionne, L. C. Kimerling, and C. A. Ross, Nat. Photonics **5**, 758 (2011).

[37]W. Yan, Y. Yang, S. Liu, Y. Zhang, S. Xia, T. Kang, W. Yang, J. Qin, L. Deng, and L. Bi, Optica **7**, 1555 (2020).

[38]X. Zhou, X. Lin, Z. Xiao, T. Low, A. Alù, B. Zhang, and H. Sun, Phys. Rev. B **100**, 115429 (2019).

[39]G. Puentes, K. Y. Bliokh, C. T. Samlan, C. Prajapati, N. K. Viswanathan, and F. Nori, Optica **3**, 1039 (2016).

[40]K. Y. Bliokh, F. J. Rodríguez-Fortuño, F. Nori, and A. V. Zayats, Nat. Photonics **9**, 796 (2015).

[41]M. Kucera, J. Bok, and K. Nitsch, Solid State Commun. **69**, 1117 (1989).

[42]Y. Xu, H. Yang, Y. Zhang, G.-Y. Zhang, X. You, and Y. Jie-Hui, J. Phys.: Condens. Matter **5**, 8927 (1993).

[43]M. C. Onbasli, L. Beran, M. Zahradník, M. Kucera, R. Antoš, J. Mistrík, G. F. Dionne, M. Veis, and C. A. Ross, Sci. Rep. **6**, 23640 (2016).

[44]Y. Amnon and Y. Pochi, *Optical Waves in Crystals: Propagation and Control of Laser Radiation* (Wiley, 1984).

[45]H. A. Haus, *Waves and Fields in Optoelectronics* (Prentice Hall, 1984).

[46]A. Yariv, IEEE J. Quantum Electron. **9**, 919 (1973).

[47]Y. Kawaguchi, S. Guddala, K. Chen, A. Alù, V. Menon, and A. B. Khanikaev, arXiv:2007.14934 (2020).